01 Sep 1975

Unidimensional Turbulence in a Sheet Flow Under Rainfall - A Stochastic Analysis

H. L. Shahabian

A. Giorgini

J. W. Delleur

A. R. Rao

UNIDIMENSIONAL TURBULENCE IN A SHEET FLOW UNDER RAINFALL - A STOCHASTIC ANALYSIS

H. L. Shahabian, Aldo Giorgini,
J. W. Delleur, A. R. Rao
School of Civil Engineering
Purdue University
Lafayette, Indiana

ABSTRACT

Probability distributions of longitudinal velocity fluctuations are presented for cases with and without rainfall. They deviate from the normal distribution. These velocity fluctuations are fitted by an autoregressive - moving average process. The process explains adequately the variance of the series.

EXPERIMENTAL SET-UP

The data analyzed are the output from a hot-film sensor positioned at different depths in a shallow water flow field where rainfall can be superimposed. The apparatus consists of a smooth plexiglass surface that acts as a catchment on which constant discharges can be obtained. A uniform rainfall can be superimposed on this surface by an independent system. The measurements are done by means of a hot-film sensor the output of which is recorded on analog magnetic tape for approximately two (2) minutes and later digitized at the rate of .003 seconds. The digitized data in turn are recorded on magnetic tape for further analysis. The apparatus, electronic data collection and processing were described in detail by Kisisel, et.al. (1, 2), whose data are used in this paper.

The longitudinal velocity fluctuations of two (2) cases are presented: one with and the other without rainfall. For comparison, the two (2) cases have very close Reynolds numbers (≈ 10,000); the parameters of the flow fields are given in Figures 1 and 2.

DETERMINATION OF THE SAMPLING INTERVAL

A digitization rate of .003 seconds was used initially to discretize the continuous signal, this rate being the maximum attainable by the available hybrid facilities. However, this rate was soon found to be too high and the number of data points was too large. For the purpose of studying the probability distribution of the turbulence signal the sampling rate can be reduced without loss of valuable information. The effects of two (2) digitization rates can be compared by calculating the eigenvalues of the autocorrelation matrices for the two (2) digitization rates. If the additional eigenvalues resulting from higher sampling rate are small, the lower sampling rate can be taken as adequately representing the series. However, the computation of eigenvalues is time consuming. Fukunaga (3) defines a criterion, J_n, which is an approximate ratio of the sum of n smaller eigenvalues of the autocorrelation matrix to the sum of all 2n eigenvalues. For stationary series J_n could be calculated by

$$J_n = \tfrac{1}{2}\{R(0) - R(T/2n)\}/R(0)$$

where,

2n = original number of sample points
R(m) = autocorrelation function at lag m
T = time length of the series.

if $J_n \ll 1$, then n sample points can be taken instead of 2n.

This criterion, applied to the data analyzed, led to a sampling rate of .012 seconds, with very small values of J_n.

PROBABILITY DISTRIBUTION

A total of 8192 (or 2^{13}) sampling points are obtained from each data set of 98.3 seconds with an interval of .012 seconds. The frequency histograms of the turbulent velocities, so sampled, are shown in Figures 1 and 2. These curves were obtained for thirty (30) equal class intervals over the range of the data. For comparison purposes the abscissa is standardized by subtracting the mean from the actual value and dividing the result by the standard deviation. The inserted Table gives the values of the mean, variance, skewness coefficient and kurtosis of the series as well as the point mean velocity $\bar{U}$. Tables, 1a and 1b, give these four statistics of the series for different sampling intervals; the insensitivity of these parameters to the sampling rate is apparent.

Attempts were made to fit several theoretical probability distributions to the data. Table 2 summarizes the result of the χ^2 goodness of fit test. It can be seen from Table 2 that:

(1) None of the distributions considered fit the data consistently.

(2) The data with rainfall are more likely to be fitted by a theoretical probability distribution than those without rainfall.

(3) Whenever the parameters converge a Pearson type 4 probability distribution fits the data.

(4) A log-normal distribution is an adequate "runner-up."

STOCHASTIC ANALYSIS

The standardized data are treated as time series. The Fast Fourier Transform (FFT) algorithm is used to obtain raw periodograms which are then averaged over eight (8) consecutive series to obtain an estimate of the power spectrum with a frequency resolution of .0814 cps and a Nyquist frequency of 41.66 cps. The equivalent number of degrees-of-freedom for the approximating χ^2 distribution of the average power spectrum is sixteen (16). The autocorrelation function is calculated by taking the inverse Fourier transform of the spectrum. The spectra and autocorrelation functions for alternating series are presented in Figures 3, 4, 5, and 6. In Figures 3 and 4 the spectra are presented up to 20.833 cps, half the Nyquist frequency. The spectra are decreasing uniformly between 20.83 cps and 41.66 cps. The autocorrelation functions, on the other hand, are presented in Figures 5 and 6 in their entirety (up to 6.144 seconds).

These functions are smooth but oscillatory around zero (0) for small values of y/d; the fluctuations increase with an increase of the y/d value (away from the wall). The spectra, on the other hand, are relatively large for low frequencies and decrease rapidly to zero (0) at about ¼ of the Nyquist frequency. Except for random changes of the fluctuating peaks they do present a similar shape over the range of y/d analyzed. This shape of the spectrum suggests an autoregressive - moving average (ARMA) type of process, Shahabian (5).

FROM BURGERS' EQUATION TO ARMA PROCESS

Since the Navier-Stokes equations contain second order space derivatives and a mean velocity, with respect to which the velocity fluctuations are small, an autoregressive process of the second order, AR(2), may be suspected to be a strong component of the process under investigation.

In this respect, an argument based on the Burgers' equation, a one-dimensional model for analytic studies on turbulence, is presented.

$$\frac{\partial U}{\partial t} + U \frac{\partial U}{\partial x} = \nu \frac{\partial^2 U}{\partial x^2} \qquad (1)$$

Decomposing the velocity U into an average and a fluctuating component

$$U = \bar{U} + u$$

equation (1) can be rewritten as

$$\frac{\partial u}{\partial t} + \bar{U} \frac{\partial u}{\partial x} + u \frac{\partial u}{\partial x} = \nu \frac{\partial^2 u}{\partial x^2} \qquad (2)$$

A finite difference form of (2) with

$$U_n(\tau) = u(n\Delta x, \tau\Delta t)$$

becomes:

$$\frac{U_n(\tau + 1) - U_n(\tau - 1)}{2\Delta t} + \left[\bar{U} + U_n(\tau)\right] \frac{U_{n+1}(\tau) - U_{n-1}(\tau)}{2\Delta x} = \nu \left[\frac{U_{n+1}(\tau) - 2U_n(\tau) + U_{n-1}(\tau)}{\Delta x^2}\right] \qquad (3)$$

stipulating that Δt and Δx are related via $\bar{U}$ as

$$\bar{U} = \frac{\Delta x}{\Delta t}$$

define the nondimensional quantities

$$V_n(\tau) = \frac{U_n(\tau)}{\bar{U}} \quad ; \quad R = \frac{\bar{U}\Delta x}{\nu} = \frac{\bar{U}^2 \Delta t}{\nu}$$

and let $a_n(\tau)$ be defined by

$$V_{n+1}(\tau + 1) = V_n(\tau) + a_n(\tau) \qquad (4)$$

where $a_n(\tau)$ represents the unsteady component of the turbulent fluctuations as seen by an observer moving with velocity $\bar{U}$; (Note that: if $a_n(\tau) \equiv 0$, Equation (4) reduces to the Taylor's hypothesis). Replacing the nondimensional quantities defined, and reducing

the velocity fluctuations to the point n making use of (4), Equation (3) becomes:

$$V_n(\tau + 1)\left[1 + \frac{R}{2} V_n(\tau)\right] - 2\, V_n(\tau) + V_n(\tau - 1)\left[1 - \frac{R}{2} V_n(\tau)\right] = a_{n-1}(\tau)\left[\frac{R}{2}\{1 + V_n(\tau)\} + 1\right] + a_n(\tau - 1)\left[\frac{R}{2}\{1 + V_n(\tau)\} - 1\right] \quad (5)$$

whose linearized form is:

$$V_n(\tau + 1) - 2\, V_n(\tau) + V_n(\tau - 1) = a_{n-1}(\tau)\left[1 + \frac{R}{2}\right] - a_n(\tau - 1)\left[1 - \frac{R}{2}\right] \quad (6)$$

If the $a_n(\tau)$ series is strongly correlated to the $a_{n-1}(\tau)$ series, Equation (6) may be seen as a second order autoregressive first order moving average, ARMA (2, 1), process on $V_n(\tau)$ of the form

$$x(t + 1) - \phi_1 x(t) - \phi_2 x(t - 1) = Z(t) + \theta_1 Z(t - 1) \quad (7)$$

However, if the $a_{n-1}(\tau)$ is only weakly correlated to $a_n(\tau)$, a new variable, $b_n(\tau)$, may be defined as in Equation (4):

$$a_{n+1}(\tau + 1) = a_n(\tau) + b_n(\tau) \quad (8)$$

(Note: $b_n(\tau)$ would represent the rate of change of the unsteady component of the velocity fluctuations as seen by an observer moving with velocity $\bar{U}$).

Substituting (8) in Equation (6):

$$V_n(\tau + 1) - 2\, V_n(\tau) + V_n(\tau - 1) = a_n(\tau + 1)\left[1 + \frac{R}{2}\right] - a_n(\tau - 1)\left[1 - \frac{R}{2}\right] - b_{n-1}(\tau)\left[1 + \frac{R}{2}\right] \quad (9)$$

which suggests an ARMA (2, 2) process. Analogous observations could be made for the nonlinearized difference Equation (5) if the $V_n(\tau)$ values in brackets are considered as the RMS value of the velocity fluctuations.

Thus, while the $V_n(\tau)$ process is a complex one as represented by Equation (3) in finite difference form in the case of the Burgers' equation, a strong AR (2) component seems to be present. An ARMA (2, 2) or ARMA (2, 1) model would appear to represent the system depending on the degree of correlation of the unsteady component of the velocity fluctuations at two (2) successive stations.

The actual analysis of the data shows that the parameters of the ARMA (2, 2) type process do not converge thus the ARMA (2, 1) model is used for the analysis.

FIT OF ARMA (2 ,1) MODEL

The parameters ϕ_1, ϕ_2, and θ_1 of the process (7) are calculated from the autocorrelation function of the data, following the procedure by Box and Jenkins (5). These parameters are given on Figures 5 and 6. The diagnostics of the model are performed by generating the residual series by means of

$$Z(t) = x(t) - \phi_1 x(t - 1) - \phi_2 x(t - 2) - \theta_1 Z(t - 1)$$

where the

$$x(t)$$

series is the standardized data and

$$\phi_1,\ \phi_2,\ \text{and}\ \theta_1$$

are the calculated parameters. The initial value of Z(t) is assumed to be zero (0). The variance and first order serial correlation coefficient of the residual series are calculated and are presented in Figures 7 and 8. It can be seen from these parameters that the variance of the residual series is much smaller than that of the standardized original series which has a variance of 1.00. The reduction is of the order of 85%. The reduction is much more pronounced for the small y/d values and it decreases with the increase of y/d.

The test of the model is to compare the residual series to white noise. In this respect the autocorrelation functions are calculated and they are shown in Figures 7 and 8, for the corresponding series shown previously. The autocorrelation functions decrease very rapidly to zero (0) after a lag of one (1) and oscillate around the zero (0) axis throughout the range considered with very small amplitude, which is characteristic of an uncorrelated random sequence.

The spectra of the residual series are calculated and shown in Figures 9 and 10 for the same series. The spectra are flat and oscillating around the theoretical spectrum of a white noise having the corresponding variance. A test of white noise in the frequency domain is on the cumulative spectrum with a test of significance due to Kolmogoroff and Smirnov (7). This test is shown in Figures 11 and 12 where the 75% and 95% confidence intervals are drawn together with the theoretical line. The actual data oscillate around the theoretical line and except for one series they all lie within the confidence interval showing that the noise term is free of cyclical components. The particular series that does not pass the test is due to a peak in the spectrum of the residual series at around fifteen (15) cps.

Thus an ARMA (2, 1) process gives a reasonably good fit of this particular form of turbulence and ex-

plains most of the variance of the process adequately. This particular model could be used to generate unidimensional turbulence where need be, like for example in particle diffusion problems or sediment transport process.

ACKNOWLEDGEMENT

The authors acknowledge the work of I. T. Kisisel who took the original data which are analyzed in this paper. This work was supported by the Purdue Research Foundation under grant XR-7533.

BIBLIOGRAPHY

(1) Kisisel, I. T.; Rao, R. A.; Delleur, J. W.; "Turbulence in Shallow Water Flow Under Rainfall", Journal of Engineering Mechanics Division, ASCE, Vol. 99, No. EMI, 1973.

(2) Kisisel, I. T.; Rao, R. A.; Delleur, J. W.; Meyer, L. D.; "Turbulence Characteristics of Overland Flow--The Effects of Rainfall and Boundary Roughness", Purdue Water Resources and Hydromechanics Laboratory, Technical Report No. 28, February 1971.

(3) Fukunaga, K., "Introduction to Statistical Pattern Recognition", Academic Press, 1972.

(4) Zaric, Z.; "Etude Statistique de la Turbulence Pariétale", Laboratoire de Transfert Thermique, Institut "Boris Kidric," Belgrade, Yougoslavie, 1974.

(5) Box, G. E. P.; Jenkins, G. M.; "Time Series Analysis, Forecasting and Control:, Holden - Day, 1970.

(6) Shahabian, H. L., "Spectral Analysis and Its Applications to Hydrologic Time Series of Lower Ohio Tributaries", M.S.C.E. Thesis, Purdue University, 1973.

(7) Jenkins, G. M.; Watts, D. G., "Spectral Analysis and Its Applications", Holden - Day, 1969.

(8) Tao, P. C.; "Distribution of Hydrologic Independent Stochastic Components", Ph.D. Thesis, Colorado State University, August 1973.

Table 1a--STATISTICS OF LONGITUDINAL VELOCITY FLUCTUATIONS WITHOUT RAINFALL WITH DECREASING DIGITIZATION RATE

Δt N	.003 32768	.006 16384	.012 8192	.024 4096	.048 2048	y/d
$\bar{m} \times 10^2$	.740	.740	.740	.742	.742	.020
$s^2 \times 10^2$	.148	.148	.148	.148	.148	
Skew.Coef.	.313	.313	.312	.319	.314	
Kurtosis	2.56	2.56	2.55	2.57	2.58	
$\bar{m} \times 10^2$	1.205	1.205	1.204	1.217	1.205	.179
$s^2 \times 10^2$	.424	.424	.424	.424	.418	
Skew.Coef.	.559	.558	.560	.568	.553	
Kurtosis	2.97	2.97	2.97	2.97	2.97	
$\bar{m} \times 10^2$	1.008	1.005	1.006	1.001	.977	.292
$s^2 \times 10^2$	.422	.422	.422	.420	.423	
Skew.Coef.	.609	.603	.604	.619	.648	
Kurtosis	3.56	3.55	3.56	3.55	3.69	
$\bar{m} \times 10^2$	.920	.916	.917	.942	.922	.405
$s^2 \times 10^2$	.340	.341	.341	.342	.347	
Skew.Coef.	.656	.647	.646	.638	.657	
Kurtosis	3.74	3.74	3.77	3.76	3.94	
$\bar{m} \times 10^2$	.360	.361	.361	.361	.354	.575
$s^2 \times 10^2$	.205	.205	.205	.206	.208	
Skew.Coef.	-.580	-.578	-.573	-.571	-.561	
Kurtosis	3.60	3.58	3.58	3.58	3.50	
$\bar{m} \times 10^2$	.412	.409	.410	.416	.432	.744
$s^2 \times 10^2$	.155	.155	.155	.154	.150	
Skew.Coef.	-.456	-.459	-.463	-.455	-.434	
Kurtosis	3.56	3.57	3.58	3.47	3.48	

Table 1b--STATISTICS OF LONGITUDINAL VELOCITY FLUCTUATIONS WITH RAINFALL WITH DECREASING DIGITIZATION RATE

Δt N	.003 32768	.006 16384	.012 8192	.024 4096	.048 2048	y/d
$\bar{m} \times 10^2$	.064	.064	.064	.065	.060	.012
$s^2 \times 10^2$	.011	.011	.011	.011	.011	
Skew.Coef.	.560	.560	.556	.560	.570	
Kurtosis	3.75	3.76	3.74	3.72	3.76	
$\bar{m} \times 10^2$	.827	.828	.827	.831	.826	.032
$s^2 \times 10^2$	.119	.119	.119	.119	.119	
Skew.Coef.	.764	.763	.746	.769	.768	
Kurtosis	3.84	3.84	3.84	3.83	3.83	
$\bar{m} \times 10^2$	1.657	1.660	1.661	1.660	1.639	.072
$s^2 \times 10^2$	.834	.835	.836	.838	.829	
Skew.Coef.	.710	.711	.712	.718	.730	
Kurtosis	3.40	3.40	3.40	3.41	3.44	
$\bar{m} \times 10^2$	.997	.999	1.000	1.006	.950	.123
$s^2 \times 10^2$	.644	.644	.643	.642	.651	
Skew.Coef.	.723	.724	.724	.727	.755	
Kurtosis	4.01	3.02	4.01	4.03	4.23	
$\bar{m} \times 10^2$	.282	.283	.282	.271	.278	.223
$s^2 \times 10^2$	.348	.348	.345	.347	.359	
Skew.Coef.	.390	.388	.388	.398	.422	
Kurtosis	3.73	3.72	3.72	3.73	3.72	
$\bar{m} \times 10^2$	-.209	-.208	-.203	-.213	-.241	.374
$s^2 \times 10^2$	.352	.352	.352	.350	.358	
Skew.Coef.	.467	.462	.464	.469	.517	
Kurtosis	3.79	3.78	3.76	3.73	3.76	

Table 2a--χ^2 GOODNESS OF FIT TEST OF PROBABILITY DENSITY FUNCTIONS WITHOUT RAINFALL

y/d	.020	.179	.292	.405	.575	.744
Normal	348	459	456	373	389	253
Normal Hermite - 3	208	147	90	68	90	46
Normal Hermite - 4	125	144	135	93	62	33
Log Normal	150	76	87	39	--	702
Pearson type 4	--	--	--	--	--	43
Gamma 3	153	59	121	69	--	--
Gamma 3 + Laguerre 3	86	52	78	26	--	--
Gamma 3 + Laguerre 4	2539	6922	82465	22000	--	--
Double-branch Gamma 3	1283	746	643	630	782	477
Normal + Gamma 3	289	49	--	74	--	--
Mixture 2 Normal	--	--	493	394	--	--
Mixture 3 Normal	112	378	664	714	317	397
Weibull	273	413	988	845	--	--

* Digitization Rate = .012 seconds
critical $\chi^2(99\%) = 48$

Table 2b--χ^2 GOODNESS OF FIT TEST OF PROBABILITY DENSITY FUNCTIONS WITH RAINFALL

y/d	.012	.032	.072	.123	.223	.374
Normal	237	490	547	315	98	152
Normal Hermite -3	57	121	172	88	69	38
Normal Hermite - 4	55	89	172	141	61	48
Log Normal	40	73	51	42	53	31
Pearson type 4	31	--	--	42	38	18
Gamma 3	51	92	49	40	58	38
Gamma 3 + Laguerre 3	40	78	51	36	66	34
Gamma 3 + Laguerre 4	2700	6628	5945	1558	66	34
Double-branch Gamma 3	520	432	684	613	465	442
Normal + Gamma 3	29	73	69	89	--	25
Mixture 2 Normal	205	--	--	340	42	136
Mixture 3 Normal	536	3600	1050	991	284	439
Weibull	577	550	434	515	624	729

* Digitization Rate = .012 seconds
critical $\chi^2(99\%) = 48$

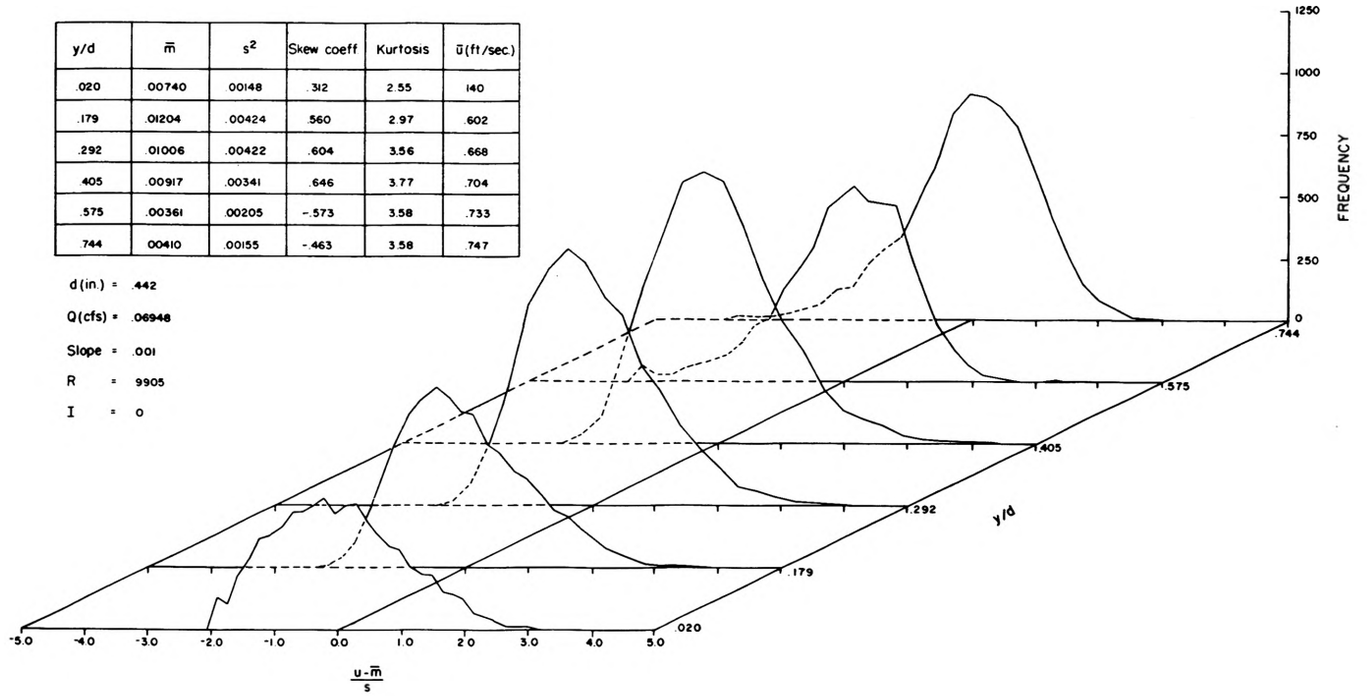

Figure 1--FREQUENCY HISTOGRAMS OF STANDARDIZED VELOCITY FLUCTUATIONS, WITHOUT RAINFALL. (y/d not to scale)

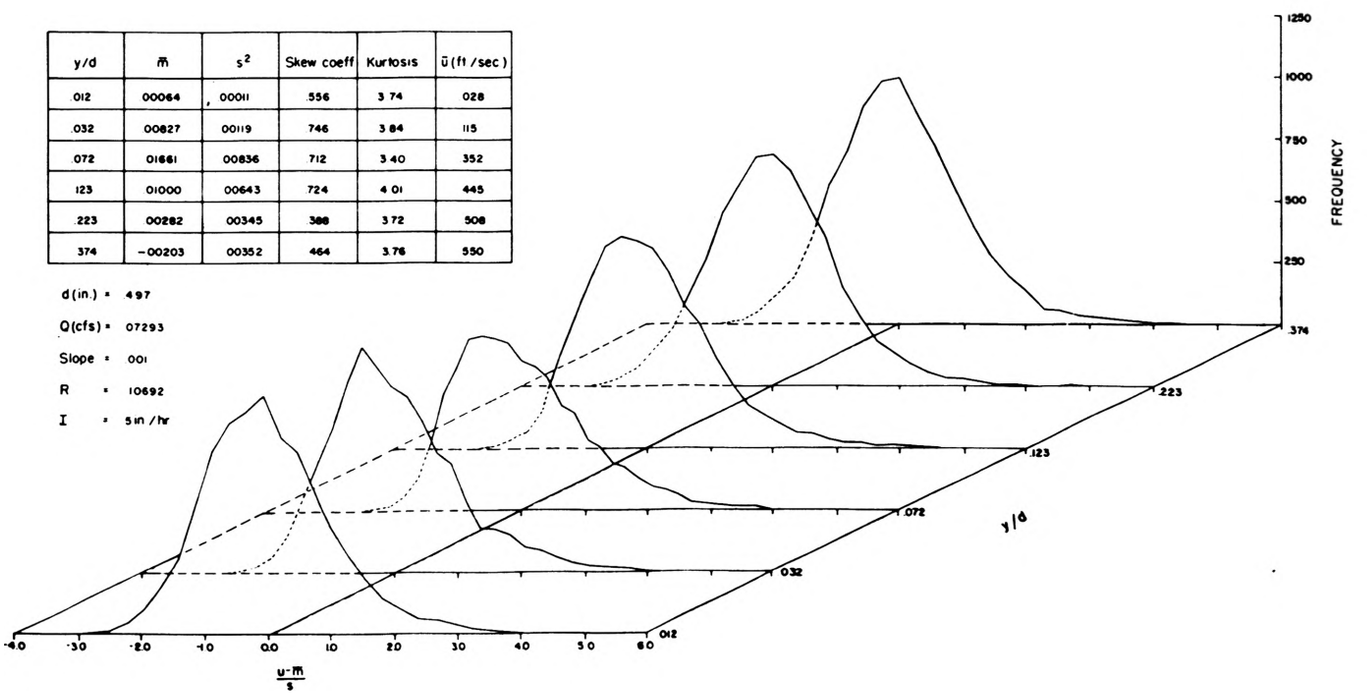

Figure 2--FREQUENCY HISTOGRAMS OF STANDARDIZED VELOCITY FLUCTUATIONS, WITH RAINFALL. (y/d not to scale)

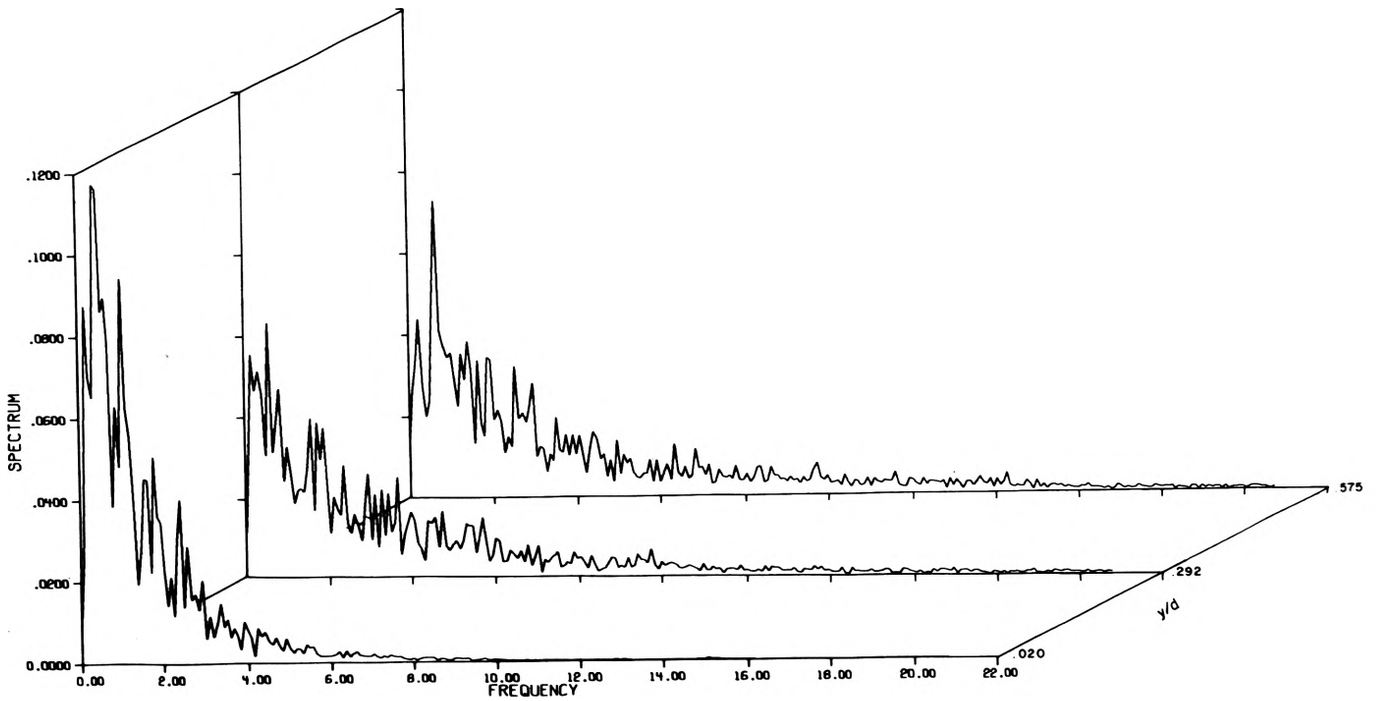

Figure 3--SPECTRA OF STANDARDIZED VELOCITY FLUCTUATIONS, WITHOUT RAINFALL.

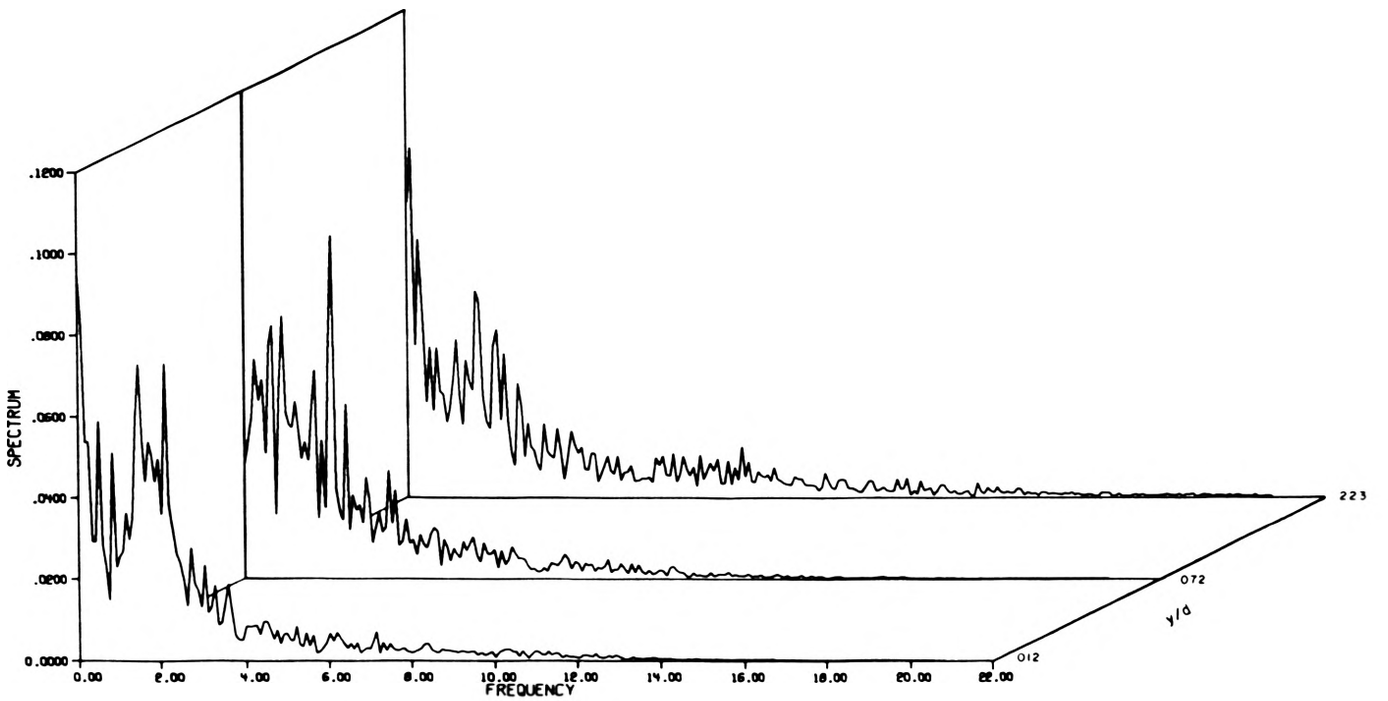

Figure 4--SPECTRA OF STANDARDIZED VELOCITY FLUCTUATIONS, WITH RAINFALL.

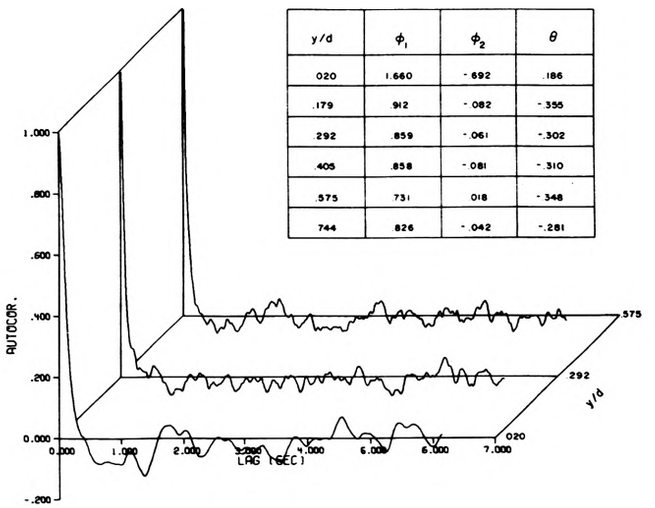

y/d	ϕ_1	ϕ_2	θ
020	1.660	- 692	.186
.179	.912	- 082	- 355
292	.859	- 061	- 302
405	.858	- 081	- 310
.575	731	018	- 348
744	826	- 042	- 281

Figure 5--AUTOCORRELATION OF VELOCITY FLUCTUATIONS, WITHOUT RAINFALL.

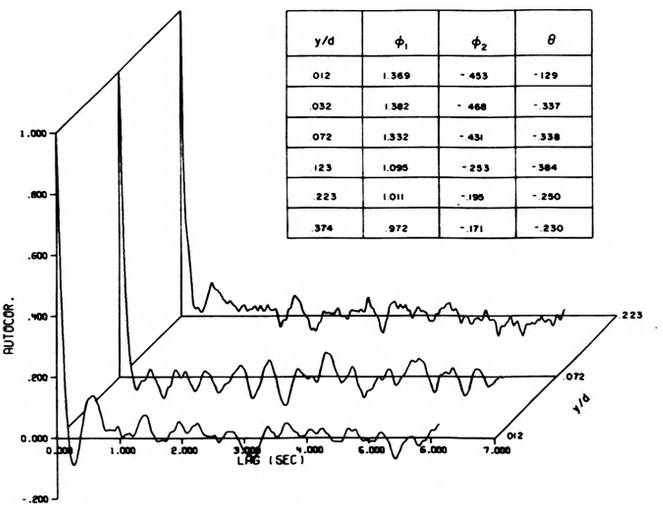

y/d	ϕ_1	ϕ_2	θ
012	1.369	- 453	- 129
032	1.382	- 468	- 337
072	1.332	- 431	- 338
123	1.095	- 253	- 384
223	1.011	- 195	- 250
374	972	- 171	- 230

Figure 6--AUTOCORRELATION OF VELOCITY FLUCTUATIONS, WITH RAINFALL.

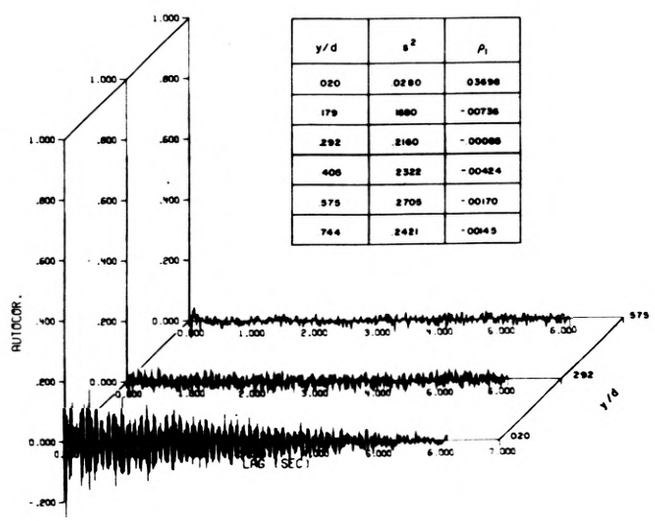

y/d	s^2	ρ_1
020	0280	03698
179	1880	- 00736
292	2160	- 00088
405	2322	- 00424
575	2705	- 00170
744	2421	- 00145

Figure 7--AUTOCORRELATION OF RESIDUALS FROM ARMA(2, 1) MODEL, WITHOUT RAINFALL.

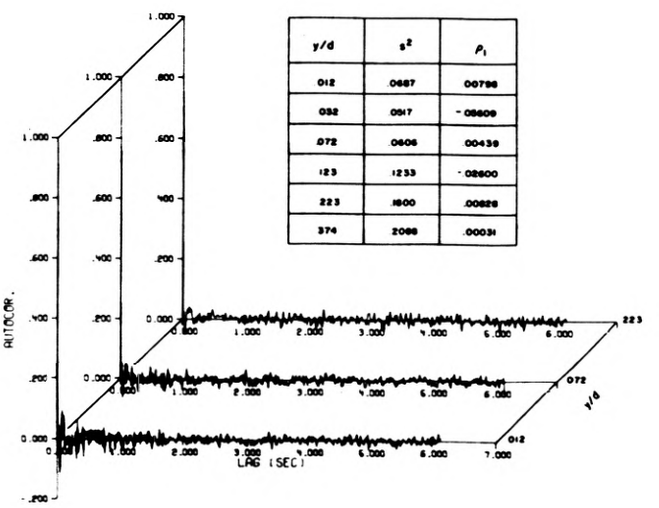

y/d	s^2	ρ_1
012	0687	00798
032	0517	- 08609
072	0606	00439
123	1233	- 02800
223	1800	.00828
374	2068	.00031

Figure 8--AUTOCORRELATION OF RESIDUALS FROM ARMA (2, 1) MODEL, WITH RAINFALL.

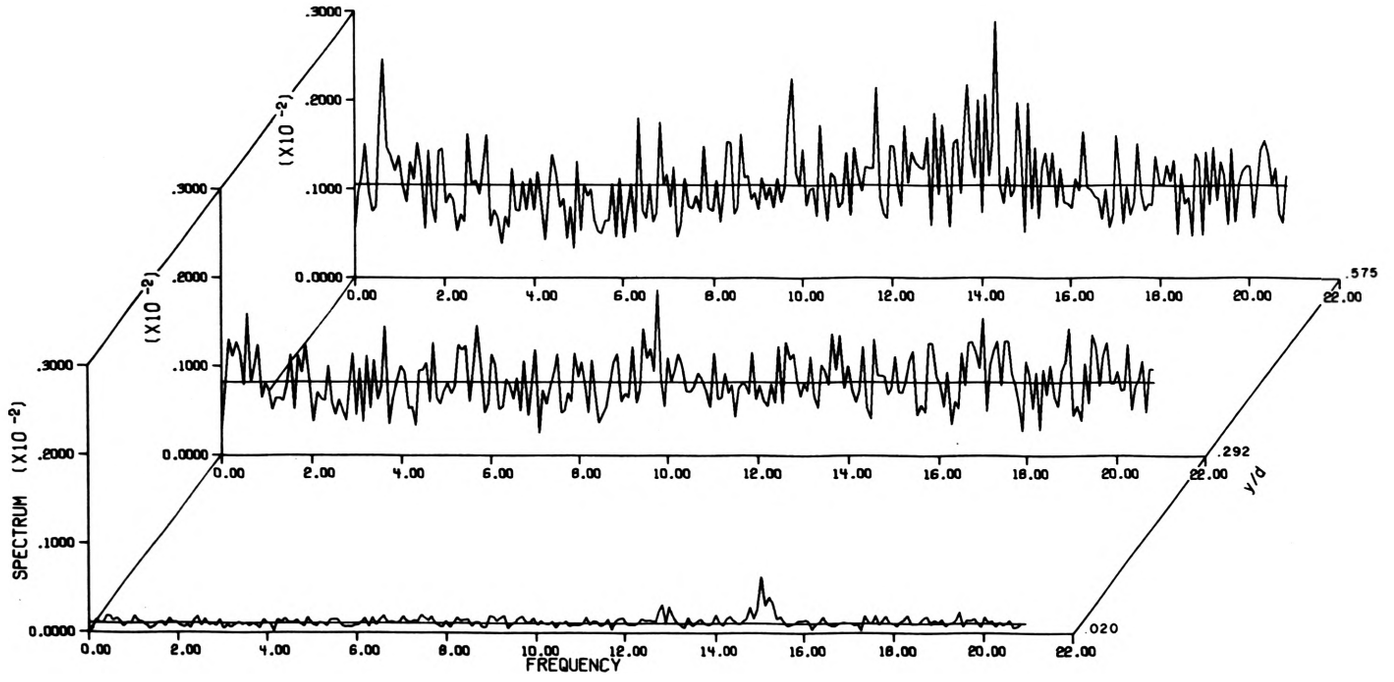

Figure 9--SPECTRA OF RESIDUALS FROM ARMA (2, 1) MODEL, WITHOUT RAINFALL.

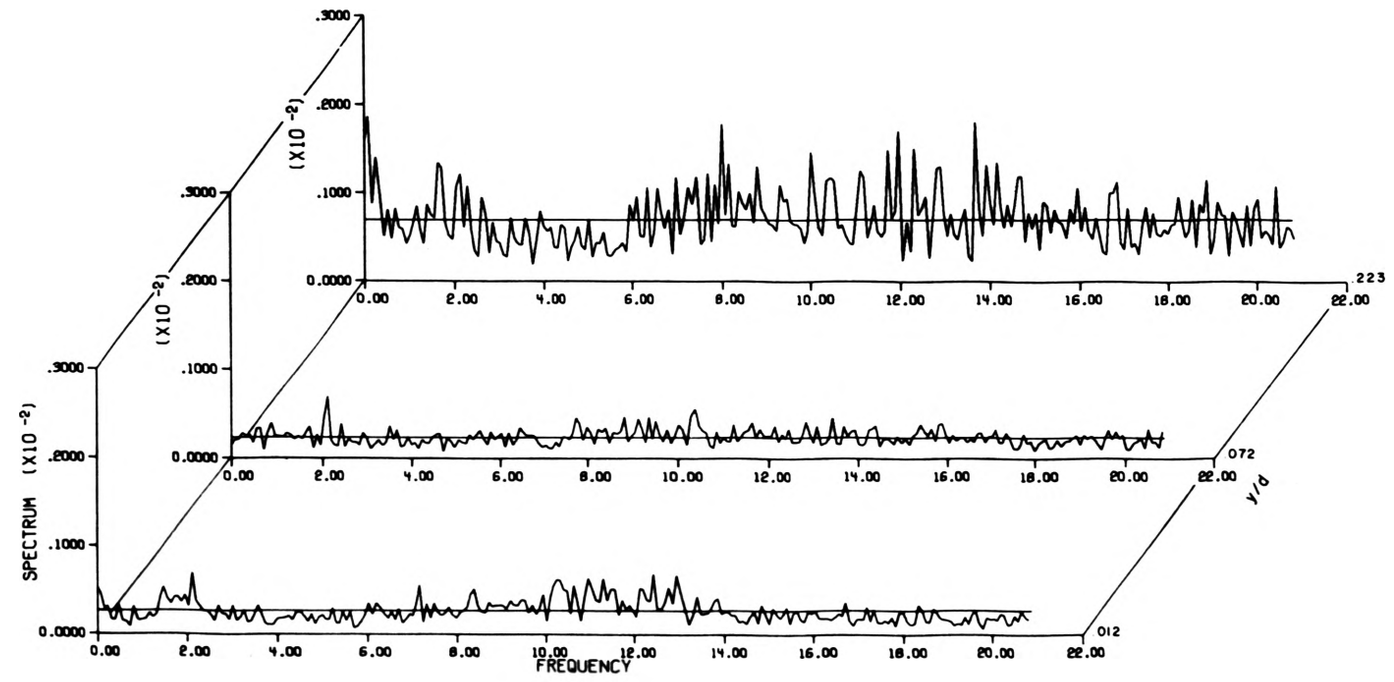

Figure 10--SPECTRA OF RESIDUALS FROM ARMA (2, 1) MODEL, WITH RAINFALL.

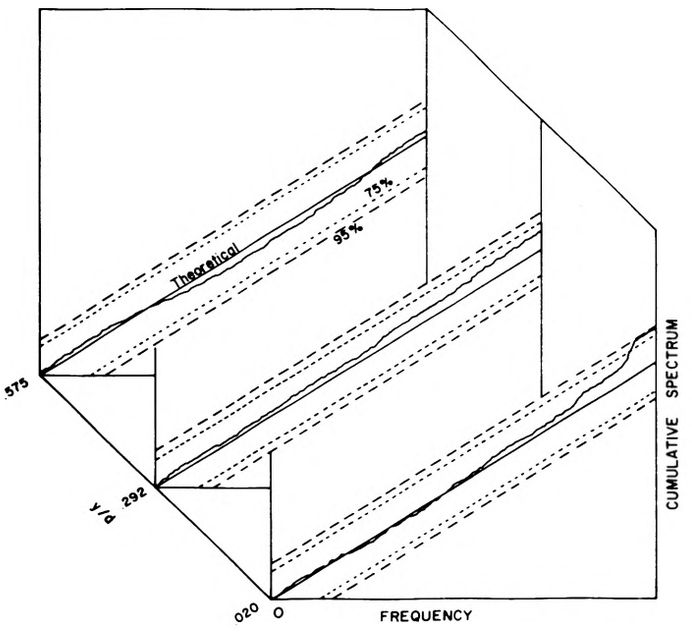

Figure 11--A TEST OF WHITE NOISE USING INTEGRATED SPECTRA OF RESIDUALS, WITHOUT RAINFALL.

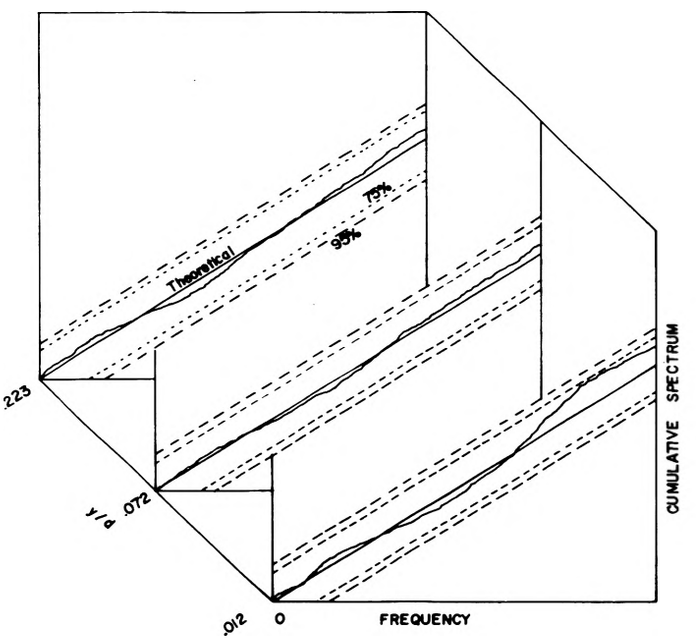

Figure 12--A TEST OF WHITE NOISE USING INTEGRATED SPECTRA OF RESIDUALS, WITH RAINFALL.

DISCUSSION

T. Hanratty, University of Illinois: I was wondering if you'd care to comment on the motivation for looking at this, with or without rainfall? Are you looking for something very different and why?

Shahabian: The motivation of the study of the turbulent flow field as generated by the impact of the rain drops over a sheet flow is mainly related to erosion. This model allows the generation of this type of turbulent flow field. Now, for the overland flow we have very shallow water and usually we don't have significant turbulence if rainfall is not present. However when the rainfall is superimposed large eddies are formed and we have an artiticially created turbulence in the flow field, and this is where the interest comes from.

W. Blake, Naval Ship Research and Development Center: What is an auto-regressive quantity?

Shahabian: An auto-regressive process is one whereby the element in a time series at a given time is related to elements of the series at previous times:

$$X(t) = \phi_1 x(t-1) + \phi_2 x(t-2) \ldots \phi_n x(t-n) + Z(t)$$